Title

Effects of nitrate on the treatment of lead contaminated groundwater by nanoscale zerovalent iron

Authors

Su, Yiming
Adeleye, Adeyemi S
Zhou, Xuefei
et al.

Publication Date

2014-09-01

DOI

10.1016/j.jhazmat.2014.08.040

Peer reviewed

Journal of Hazardous Materials 280 (2014) 504–513

Contents lists available at ScienceDirect

Journal of Hazardous Materials

journal homepage: www.elsevier.com/locate/jhazmat

Effects of nitrate on the treatment of lead contaminated groundwater by nanoscale zerovalent iron

Yiming Su[a,b,c], Adeyemi S. Adeleye[b,c], Xuefei Zhou[a], Chaomeng Dai[a,d], Weixian Zhang[a], Arturo A. Keller[b,c,*], Yalei Zhang[a,**]

[a] State Key Laboratory of Pollution Control and Resources Reuse, Tongji University, Shanghai 200092, China
[b] Bren School of Environmental Science & Management, University of California, Santa Barbara, 3420 Bren Hall, CA 93106, USA
[c] University of California Center for Environmental Implications of Nanotechnology, Santa Barbara, CA, USA
[d] College of Civil Engineering, Tongji University, Shanghai 200092, China

HIGHLIGHTS

- Pb(II) removal capacity of nZVI was greatly influenced by nitrate.
- Nitrate reduction led to the formation and deformation of Pb-containing ferrite.
- ORP can indicate the transformation of nZVI particles and related redox processes.
- Shortening reaction time or adding fresh nZVI can reduce the negative effects of nitrate.

GRAPHICAL ABSTRACT

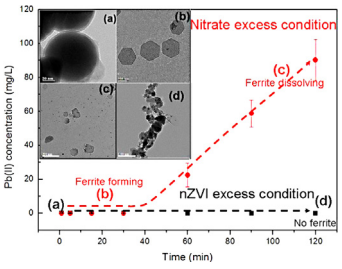

ARTICLE INFO

Article history:
Received 9 May 2014
Received in revised form 31 July 2014
Accepted 24 August 2014
Available online 30 August 2014

Keywords:
Nanoscale zerovalent iron
Lead pollution
Nitrate influence
Ferrite process
Oxidation–reduction potential

ABSTRACT

Nanoscale zerovalent iron (nZVI) is efficient for removing Pb^{2+} and nitrate from water. However, the influence of nitrate, a common groundwater anion, on Pb^{2+} removal by nZVI is not well understood. In this study, we showed that under excess Fe^0 conditions (molar ratio of Fe^0/nitrate > 4), Pb^{2+} ions were immobilized more quickly (<5 min) than in nitrate-free systems (~15 min) due to increasing pH. With nitrate in excess (molar ratio of Fe^0/nitrate < 4), nitrate stimulated the formation of crystal $Pb_xFe_{3-x}O_4$ (ferrite), which provided additional Pb^{2+} removal. However, ~7% of immobilized Pb^{2+} ions were released into aqueous phase within 2 h due to ferrite deformation. Oxidation–reduction potential (ORP) values below −600 mV correlated with excess Fe^0 conditions (complete Pb^{2+} immobilization), while ORP values ≥−475 mV characterized excess nitrate conditions (ferrite process and Pb^{2+} release occurrence). This study indicates that ORP monitoring is important for proper management of nZVI-based remediation in the subsurface to avoid lead remobilization in the presence of nitrate.

1. Introduction

Groundwater has long been used as a drinking water resource in parts of China and many other countries [1–4], but the presence of pollutants in groundwater is a common problem [1,5,6]. Nanoscale zerovalent iron (nZVI) has been extensively considered for *in situ* groundwater remediation [7–10] of a wide range of groundwater pollutants including chlorinated solvents [11,12], chlorinated pesticides [13], heavy metals [14–16], and nitrate [17–19].

* Corresponding author at: Bren School of Environmental Science & Management, University of California, Santa Barbara, 3420 Bren Hall, CA 93106, USA. Tel.: +1 8058937548; fax: +1 8058937612.
** Corresponding author. Tel.: +86 2165982503; fax: +86 2165988885.
E-mail addresses: keller@bren.ucsb.edu, arturo.keller@gmail.com (A.A. Keller), zhangyalei@tongji.edu.cn (Y. Zhang).

http://dx.doi.org/10.1016/j.jhazmat.2014.08.040
0304-3894/

Pb^{2+} is immobilized by nZVI mainly through sorption and co-precipitation and partly by reduction [15]. Nitrate removal by nZVI generally occurs via reduction to ammonium (Eq. (1)) at very high rate (50 ppm nitrate could be reduced by 1.43 g/L nZVI within 1 h, as modeled by pseudo-first-order reaction kinetics), even at high pH (9–10) [19–21]. Although there are several studies on the use of nZVI for cleanup of Pb^{2+} [22–24] or nitrate contamination [18,19] individually, little attention has been paid to the treatment of groundwater with different levels of Pb^{2+} and nitrate, even though some researchers recommend that studies need to be done in the systems similar to the real environment [25,26]. Pb^{2+} pollution results mainly from leakage of leaded gasoline and poor management of wastes from industrial processes such as mining, coal burning, battery production, and smelting [27], while nitrate contamination is mainly from fertilizer application, irrigation with untreated wastewater, and industrial processes [2,28]. Nitrate concentrations as high as 300 mg/L have been detected in groundwater [2].nZVI is easily oxidized on exposure to water, hence the Fe(0) core is surrounded by an oxide layer [6,29]. The core-shell structure is key for Pb^{2+} sequestration (partly reduction by core but mainly adsorption and co-precipitation on shell) [15,29,30], but this unique structure is destroyed during the nitrate reduction process as Fe(0) may be oxidized completely [19]. The potential effect of the damaged structure on the ability of nZVI to immobilize Pb^{2+} has not been investigated to date.

Nitrate reduction by nZVI (Eq. (1)) will increase solution pH (to <10) from the accumulation of hydroxyl ions [19,31], which could possibly enhance heavy metal removal through precipitation and the ferrite formation process (Eqs. (2) and (3)) [32,33]. As shown in Eq. (2), Pb^{2+} ions may be incorporated into the lattice points of ferrites ($Pb_xFe_{3-x}O_4$) during their formation through co-precipitation [32]. Ferrite formation occurs mainly via oxidation of Fe^{2+} at high pH and temperature in the presence of an oxidant (Eq. (2)) [32]. Although dissolved oxygen can be limited or even non-existent in nZVI reaction systems (which means Eq. (2) is not likely to happen), nitrate also could oxidize Fe^{2+} to Fe^{3+}, leading to the formation of $Pb_xFe_{3-x}O_4$ (Eq. (3)). Therefore, nitrate reduction by nZVI may result in both negative (damage of core-shell structure) and positive (high pH and ferrite formation) effects on Pb^{2+} immobilization.

$$NO_3^- + 4Fe^0 + 7H_2O \rightarrow 4Fe^{2+} + NH_4^- + 10OH^- \quad (1)$$

$$xPb^{2+} + (3-x)Fe^{2+} + 6OH^- + 0.5O_2 \rightarrow Pb_xFe_{(3-x)}O_4 + 3H_2O \quad (2)$$

$$2Fe^{3+} + (1-x)Fe^{2+} + xPb^{2+} + 8OH \xrightarrow{NO_3^-, NO_2^-} Pb_xFe_{(3-x)}O_4 + 4H_2O \quad (3)$$

An important parameter to be considered in nZVI-based remediation (when it occurs via adsorption, such as Pb^{2+}) in the presence of groundwater oxidants (e.g. nitrate) is the amount of nZVI to be applied. Due to oxidation, nZVI may persist for less time when oxidants are abundant in the environment than when oxidants are limited [7,34,35]. If all nZVI is consumed by nitrate and/or other oxidants, previous adsorbed/co-precipitated Pb^{2+} on the surface of nZVI will be likely released into solution again. Consequently, to avoid possible remobilization of pollutants (e.g. Pb^{2+}), excess nZVI (relative to oxidants) in permeable reactive barriers or injection wells is required. Oxidation and reduction potential (ORP) measurement of media, which can represent the sum of two or more redox couples [36] (such as, Fe/Fe^{2+}, H_2/H^+, NH_4^+/NO_3^-), presents a useful technique for monitoring nZVI reactivity in the subsurface and has been widely used by other studies [37–39]. ORP was successfully used to indicate the presence of Fe^0 in columns packed with hexavalent chromium, nitrate, sulfate, and trichloroethene-contaminated mixture in groundwater [40]. Shi et al. [38] showed that the specific transformation of nZVI can be effectively characterized by the ORP value of media, especially at low levels of unreacted nZVI.

In this study, we investigated nZVI remediation of lead in the presence of nitrate by carefully tracking nitrate, ammonium, nitrite, and Pb^{2+} concentrations in the aqueous phase. Transformation of nZVI and the ferrite process were also visualized via transmission electron microscopy (TEM). Furthermore, ORP monitoring was also employed to understand the reactions occurring among nZVI, Pb^{2+}, and nitrate. The results of this study provide useful information for proper management of nZVI-based remediation of lead (and possibly other heavy metals) in the presence of groundwater anions such as nitrate.

2. Material and methods

2.1. Chemical reagents

Analytical-grade lead acetate ($Pb[CH_3COO]_2{\cdot}3H_2O$, denoted as $Pb(AC)_2$), lead nitrate ($Pb(NO_3)_2$), sodium borohydride ($NaBH_4$, 98%), sodium nitrate ($NaNO_3$), and anhydrous ferric chloride ($FeCl_3$) were purchased from Aladdin (Shanghai, China). All chemicals were used without further purification.

2.2. nZVI synthesis method

nZVI was synthesized via the reaction shown in Eq. (4) [30]:

$$4Fe^{3+} + 3BH_4^- + 9H_2O \rightarrow 4Fe^0 + 3H_2BO_3^- + 6H_2 + 12H^+ \quad (4)$$

Sodium borohydride ($NaBH_4$, 0.25 M) was titrated (1 L/h) into ferric chloride solution ($FeCl_3$, 0.048 M) at a volumetric ratio of 1:1. After reduction, the jet-black iron nanoparticles were collected and washed with deionized (DI) water and anhydrous ethanol three times each. A neodymium iron boron magnet was then used to remove nZVI from suspension. Freshly prepared nZVI was stored in anhydrous ethanol solution at 4 °C until use. DI water was used in this study, and it was degassed by N_2 (final DO < 0.1 mg/L) prior to use.

2.3. Pb^{2+} removal from $Pb(NO_3)_2$ and $Pb(AC)_2$ systems using nZVI

Preliminary studies to understand Pb^{2+} sorption by nZVI from $Pb(AC)_2$ and $Pb(NO_3)_2$ were done via batch sorption experiments. The tests were carried out in a series of 100 mL conical flasks sealed with screw caps. 100 mL of sample volume was used to ensure minimal headspace; N_2 was introduced into the headspace before sealing the flasks (each flask was sampled only once to avoid reaeration). 0.25 g/L nZVI was used for all the studies while Pb^{2+} concentration was 0.97–1.93 mM. The flasks were agitated vigorously on a shaker table (200 rpm) at 25 °C, and aliquots were collected from the supernatant at different times within 2 h (preliminary experiments indicated 2 h was long enough to achieve equilibrium). Dissolved lead and iron in collected samples were determined by inductively coupled plasma (ICP; Agilent 720ES, Japan) after filtering with 0.22 μm filter and acidifying with 4% ultrahigh-purity HNO_3.

2.4. Relationship between Pb^{2+} removal and ORP in $Pb(NO_3)_2$ or $Pb(AC)_2$ reaction system

2 g/L nZVI was exposed to a series of Pb^{2+} (from $Pb(NO_3)_2$ or $Pb(AC)_2$) concentrations (1.45, 2.40, 3.85, 4.83, 5.80, 7.25, and 9.65 mM) in a three-necked flask under argon (Ar) atmosphere (Fig. S1). ORP was monitored every minute for 2 h using a HACH Sc200 (Loveland, CO). Pb^{2+} removal was determined via ICP

analysis of Pb^{2+} in supernatant as described previously. The reaction temperature was kept at 25 °C with a water bath.

2.5. Reactions among Pb^{2+}, NO_3^-, and nZVI at different nitrate abundance conditions

Reactions between $Pb(NO_3)_2$ (Pb^{2+} and NO_3^-) and nZVI were investigated under (1) excess nZVI (molar ratio of Fe^0/nitrate > 4); (2) balanced nZVI-NO_3^- (Fe^0/nitrate, ~4), and (3) excess NO_3^- (Fe^0/nitrate < 4) conditions. nZVI stock suspension was introduced to solutions with different $Pb(NO_3)_2$ concentrations in a three-necked flask under Ar atmosphere (nZVI, 500 mg/L). $Pb(NO_3)_2$ concentrations used were 0.97 mM (excess nZVI), 1.45 mM (approximately balanced nZVI-NO_3^-), and 1.93 mM (excess NO_3^-). The flask was agitated by an electric stirrer (250 rpm) at 25 °C. ORP and pH were also monitored every minute using the HACH Sc200 throughout the reaction (2 h). 1 ml of aliquots were collected in time series and analyzed for NO_3^-, NO_2^-, NH_4^+, Fe^{2+}, and Pb^{2+}. All nitrogen-containing groups were assessed via UV–Vis spectrophotometry (Shimadzu UV-2550, Japan) according to a previous study [41]. TEM analyses were also done as explained later.

2.6. Effect of NO_3^- on Pb^{2+} removal

To verify the effect of NO_3^- on Pb^{2+} removal performance of nZVI, a certain amount of nZVI stock suspension was charged into 1.2 mM $Pb(AC)_2$ solution with 0, 0.3, 0.6, 0.9, 1.2, and 1.5 mM $NaNO_3$ to achieve a final nZVI concentration of 0.2 g/L. After 20 min shaking at 200 rpm, 1 ml of aliquots was collected for Fe^{2+} and Pb^{2+} analyses via ICP as described earlier. Final pH was also measured in all the samples.

2.7. Determining nZVI re-dosing via ORP measurement

In order to approximate the right time to dose new nZVI during Pb^{2+} remediation in the presence of NO_3^-, 500 mL of 0.4 g/L nZVI suspension in natural groundwater from Santa Barbara, California, USA (characteristics in Table S1) was spiked with 1.7 mL of 48 mM $Pb(NO_3)_2$ every 15 min from 0 to 90 min. At 100 min, another dosing of nZVI was performed to achieve a theoretical nZVI load of 0.5 g/L. ORP was monitored throughout for 160 min.

2.8. Transmission electron microscopy (TEM) analyses

High-resolution TEM imaging was performed using a JEOL JEM 2011 operated at 200 kV. The TEM was coupled with an energy-dispersive X-ray spectrometer (EDS; Hitachi S-3000 N). For this experiment, 10 mL of sample mixture was collected using a syringe (the stainless steel needle was replaced by a fine long tube) at various times. A magnet was then used to separate solid from suspension, and the solid was transferred into anhydrous ethanol immediately. A few droplets of sample were then deposited onto a carbon-coated TEM grid in an anaerobic chamber and analyzed via TEM. The time between sampling and TEM analysis was minimized and kept constant for all samples. All tests were performed in triplicate.

3. Results

3.1. Pb^{2+} removal from $Pb(NO_3)_2$ and $Pb(AC)_2$ systems using nZVI

Pb^{2+} removal dynamics in $Pb(AC)_2$ or $Pb(NO_3)_2$ reaction systems were very different (Fig. 1). In the $Pb(AC)_2$ system, the majority of Pb^{2+} ions were immobilized upon contact with nZVI as indicated by much lower Pb^{2+} concentration detected at initial time t_0 relative to the amount added initially. Subsequently, residual Pb^{2+} ions were adsorbed at a relatively slower rate, and Pb^{2+} was undetectable after 2 h (except at initial $Pb(AC)_2$ concentration of 3.86 mM where 0.1 mM Pb^{2+} was detected). The initial removal rate of Pb^{2+} was even higher in the $Pb(NO_3)_2$ system than that in $Pb(AC)_2$ solution, with all Pb^{2+} ions appearing to be immobilized after about 15 min. However, from 20 to 120 min, Pb^{2+} ions were released back into solution in the $Pb(NO_3)_2$ system. For instance, at an initial $Pb(NO_3)_2$ concentration of 0.96 mM, aqueous Pb^{2+} was undetected after 20 min of exposure to nZVI. However, 100 min later, Pb^{2+} concentration increased rapidly to about 0.4 mM. Based on our results, nZVI's removal capacity of lead was >1600 mg/g in $Pb(AC)_2$ system, but it seemed unreasonable to determine the removal capacity in a $Pb(NO_3)_2$ system because of the release of Pb^{2+} after

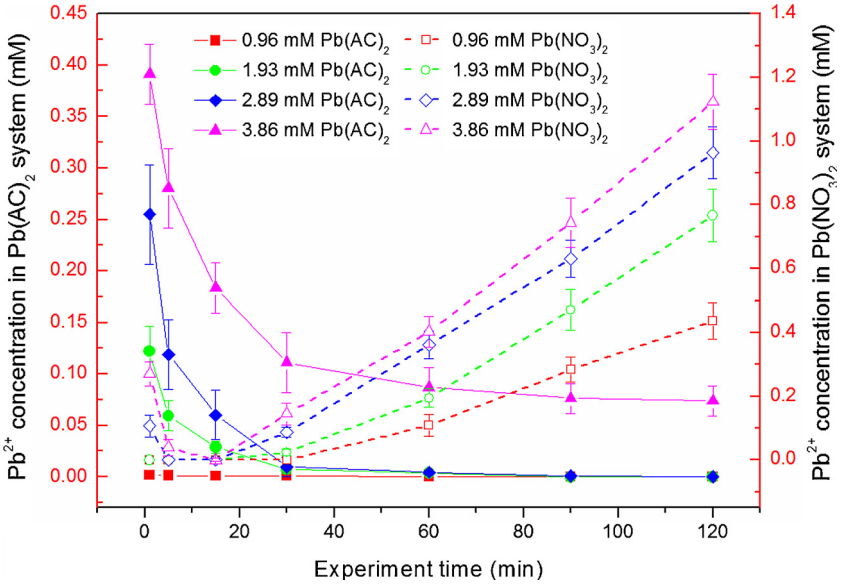

Fig. 1. Pb removal performance of nZVI (0.25 g/L) in $Pb(AC)_2$ and $Pb(NO_3)_2$ solution (error bar represents standard deviation).

initial adsorption. Clearly the presence of nitrate in groundwater will have a major effect on the ability of nZVI to remove Pb^{2+}.

3.2. Relationship between Pb^{2+} removal performance and ORP variation

To understand the relationship between ORP trend and Pb^{2+} removal performance of nZVI in the $Pb(NO_3)_2$ system, nZVI was exposed to a series of solutions with different $Pb(NO_3)_2$ concentrations and ORP was carefully monitored throughout the reaction (Fig. 2a). When the initial $Pb(NO_3)_2$ concentration was less than or equal to 3.85 mM, no Pb^{2+} ions were detected in the final supernatant (i.e. complete removal, 398 mg Pb^{2+}/g in nitrate present conditions). However, when the initial $Pb(NO_3)_2$ concentration was greater than or equal to 4.83 mM, higher concentrations of Pb^{2+} ions were detected at the end of the experiments (Fig. 2a). In Fig. 2b, the ORP curves obtained at different concentrations of $Pb(NO_3)_2$ can be divided into two main groups. The first group, corresponding to conditions with initial $Pb(NO_3)_2$ concentrations below 3.85 mM and complete removal of Pb^{2+} had a final ORP value less than −600 mV. The second group was characterized by a final ORP value around −475 mV, corresponding to the tests with initial $Pb(NO_3)_2$ concentrations above 4.83 mM. Significant amounts of Pb^{2+} ions were detected in the second group. In comparison, Pb^{2+} ions were not detected in all the conditions with $Pb(AC)_2$ as Pb^{2+} source (Fig. 2a). This implies that detection of Pb^{2+} at the end of the experiment is largely independent of initial Pb^{2+} concentrations (for the conditions of this study). Additionally, final ORP values in $Pb(AC)_2$ systems were all below −600 mV (Fig. 2c). Thus, the ORP value may be a good indicator for determining whether Pb^{2+} ions are being released or not in $Pb(NO_3)_2$-nZVI systems.

3.3. Reactions among Pb^{2+}, NO_3^-, and nZVI under different conditions

Using 0.5 g/L nZVI and 0.97, 1.45, and 1.93 mM $Pb(NO_3)_2$ resulted in three distinct conditions: excess Fe^0, balanced Fe^0-nitrate, and excess nitrate (according to Eq. (1)). Fig. 3 shows that the reactions in the three conditions can be divided into three phases, characterized by distinct ORP variation.

Under excess Fe^0 conditions (Fig. 3a and b), Pb^{2+} ions were undetected in the supernatant throughout the study. In the first phase of excess Fe^0 condition (which occurred within the first 30 min), nitrate was reduced to nitrite and ammonium, accompanied by (1) a sharp increase in pH from 7.3 to 10, and (2) a decrease in ORP to about −550 mV from about +200 mV. In the second phase, which occurred in the next 50 min, the reaction was nitrate-limited, and the accumulated nitrite was reduced by Fe^0. We only observed a slight further increase in pH and decrease in ORP compared to the first phase, as the reaction slowed down. Subsequently, pH and ORP remained constant in the third phase as nitrate and nitrite were exhausted, leaving excess Fe^0.

Similarly, there were three phases in the balanced Fe^0-nitrate conditions (Fig. 3c and d). In the first phase (first 30 min), Pb^{2+} ions were immobilized and nitrate was reduced first to ammonium, resulting in a steep increase in pH and decrease in ORP. Later, nitrite accumulation was observed, with a slight decrease in pH, while ORP reached a plateau. Adsorbed Pb^{2+} remained immobilized in this phase. During the second phase (next 30 min), ORP increased slightly to −440 mV from −650 mV while pH stabilized at ~9.2. The nitrite accumulated in the later first phase was consumed at a relatively fast rate, accompanied by a decline in Fe^{2+} concentration. In the last phase, the residual nitrite was slowly reduced and a small fraction of immobilized Pb^{2+} (~2%) was released into solution.

Under excess nitrate conditions (Fig. 3e and f), a significant amount of Pb^{2+} ions were detected at the end of the experiment. The first phase was similar to the other conditions except that initial decrease to −575 mV in ORP was quickly followed by an increase to −475 mV, all of which occurred in the first 20 min. In the second phase, pH decreased slightly followed by an increase to 9.3, while ORP decreased after an initial increase. The predominant reaction was the reduction of the accumulated nitrite, and 0.05 mM Pb^{2+} was also detected. In the last phase, residual nitrite was reduced at a slow rate and release of previously immobilized Pb^{2+} continued, but at a slower rate than in the second phase. At the end of the experiment, 0.15 mM Pb^{2+} ions were detected in solution.

Two major rapid reactions were identified in the first phase: (1) the reaction between Pb^{2+} and nZVI and (2) the reaction between nitrate and nZVI (each reduction profile from these three different conditions is fit with a first-order equation). The first reaction led to Pb^{2+} immobilization, while the second reaction resulted in the transformation of nitrate to ammonium and nitrite, and subsequently a significant increase in pH. In addition, a large amount of green rust (GR) (color of the mixture was green, and confirmed via XRD; see Fig. S2) was formed at the end of the first phase due to the formation of highly reactive Fe(II)–Fe(III) layered double hydroxides [42]. In the second phase, nitrite (formed in the first phase) was rapidly reduced by Fe^0 (in excess Fe^0 condition) or dissolved Fe^{2+}. In the last phase of excess nitrate conditions, further reduction of remaining nitrite/nitrate by Fe^{2+} in ferrite occurred, leading to the deformation of ferrite and release of immobilized Pb^{2+} back into solution. This process is discussed in detail in a later section. Although Fe^0 may also react with water, at pH above 9, the reaction rate is very small [43], which means its influence on Pb^{2+} removal performance can be neglected.

3.4. Transformation of nZVI and ferrite formation

The HR-TEM figures of iron nanoparticles isolated at different times under excess nitrate conditions (Fig. 3f) showed representative transformation of nanoparticles during the entire reaction process (Fig. 4a–d). Synthesized nZVI were almost spherical with a size range of 20–80 nm in diameter. As soon as nZVI particles were exposed to the $Pb(NO_3)_2$ solution, Fe^0 reacted with nitrate rapidly leading to increasing pH and Fe^{2+} accumulation. pH increase led to the formation of lead hydroxide (seen as tiny granules in the background of Fig. 4b) as confirmed by EDS analysis (Fig. S3 and S4). The Fe^{2+} ions produced further reacted with nitrite to produce Fe^{3+} but Fe^{2+} generation was faster than its transformation to Fe^{3+}. The presence of Fe^{3+} initiated the formation of Pb-containing ferrite crystals with diameter ≤600 nm (Fig. 4c) and thickness of ~2.58 nm (Fig. 4e). Ferrite formation is usually favored by high pH [44]. The ratio of Pb to Fe in the ferrite formed was ~0.15 as estimated by EDS (Fig. S5), and the electron diffraction pattern (Fig. 4f) confirmed that the ferrite was a hexagonal crystal system. As the reaction went on, ferrite was formed continuously because of increasing availability of Fe^{3+} (formed from Fe^{2+} oxidation by nitrite). With time, as Fe^0 and Fe^{2+} were limiting in solution (due to excess nitrate), Fe^{2+} in ferrite was used to provide electrons, causing transformation of the ferrite crystals (Fig. 4d). Under excess Fe^0 and balanced Fe^0-nitrate conditions, ferrite was not observed (Fig. S6).

3.5. Positive effect of NO_3^- on Pb^{2+} removal

Pb^{2+} removal by nZVI was significantly influenced by the presence and concentration of nitrate. In this study, Pb^{2+} removal rate reached a peak after 20 min in the $Pb(NO_3)_2$ reaction system. Here (Fig. 5a), we provided the results from experiments which were over within 20 min. Seen from Fig. 5a, while about 8% of Pb^{2+} was removed in nitrate-free conditions (final pH 5.0), almost 100% Pb^{2+} ions were sequestered when 1.2 mM nitrate was present in solution (final pH 6.4). Nitrate reduction by nZVI led to increase in solution

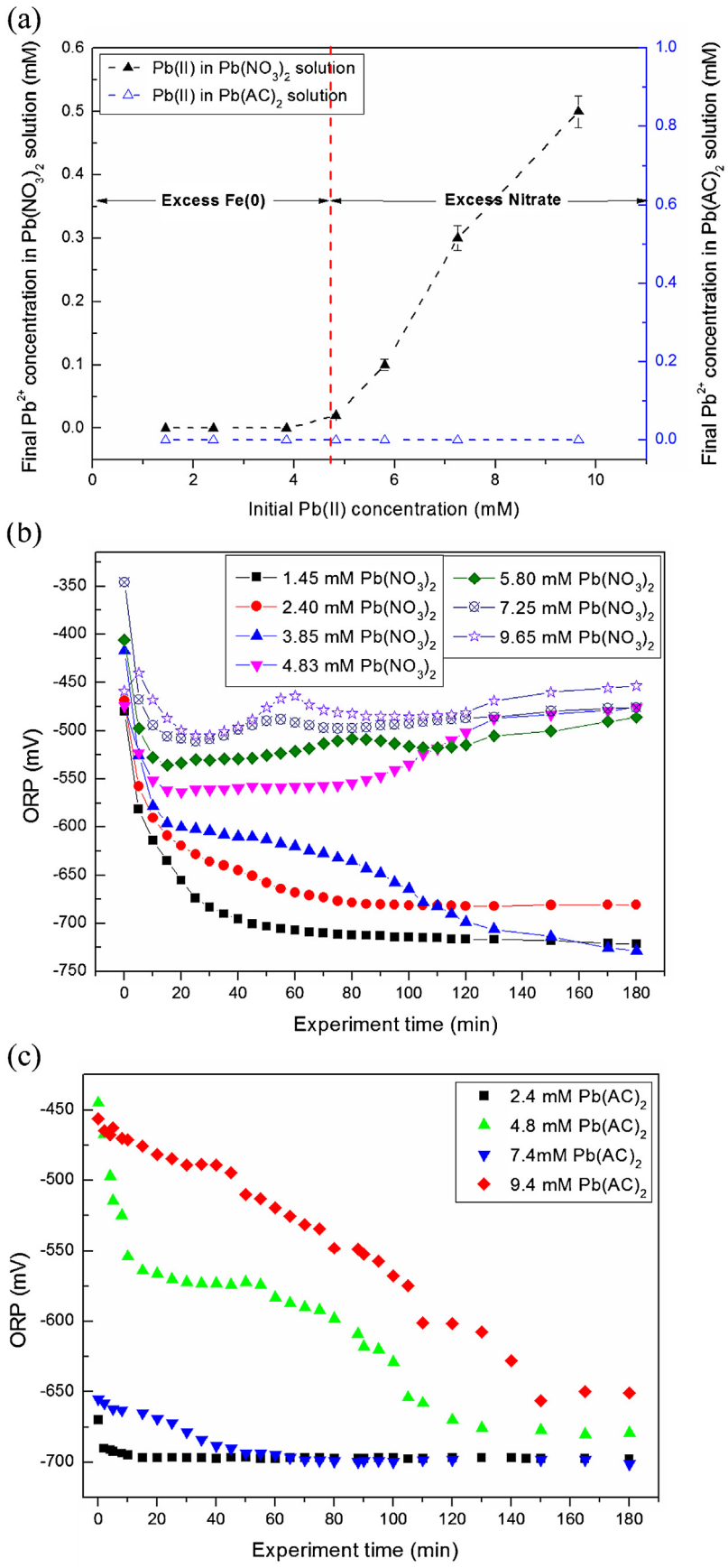

Fig. 2. (a) Final Pb(II) concentrations in $Pb(NO_3)_2$ and $Pb(AC)_2$ solutions (nZVI, 2 g/L); (b) ORP during the reaction between nZVI (2 g/L) and $Pb(NO_3)_2$; (c) ORP during the reaction between nZVI (2 g/L) and $Pb(AC)_2$.

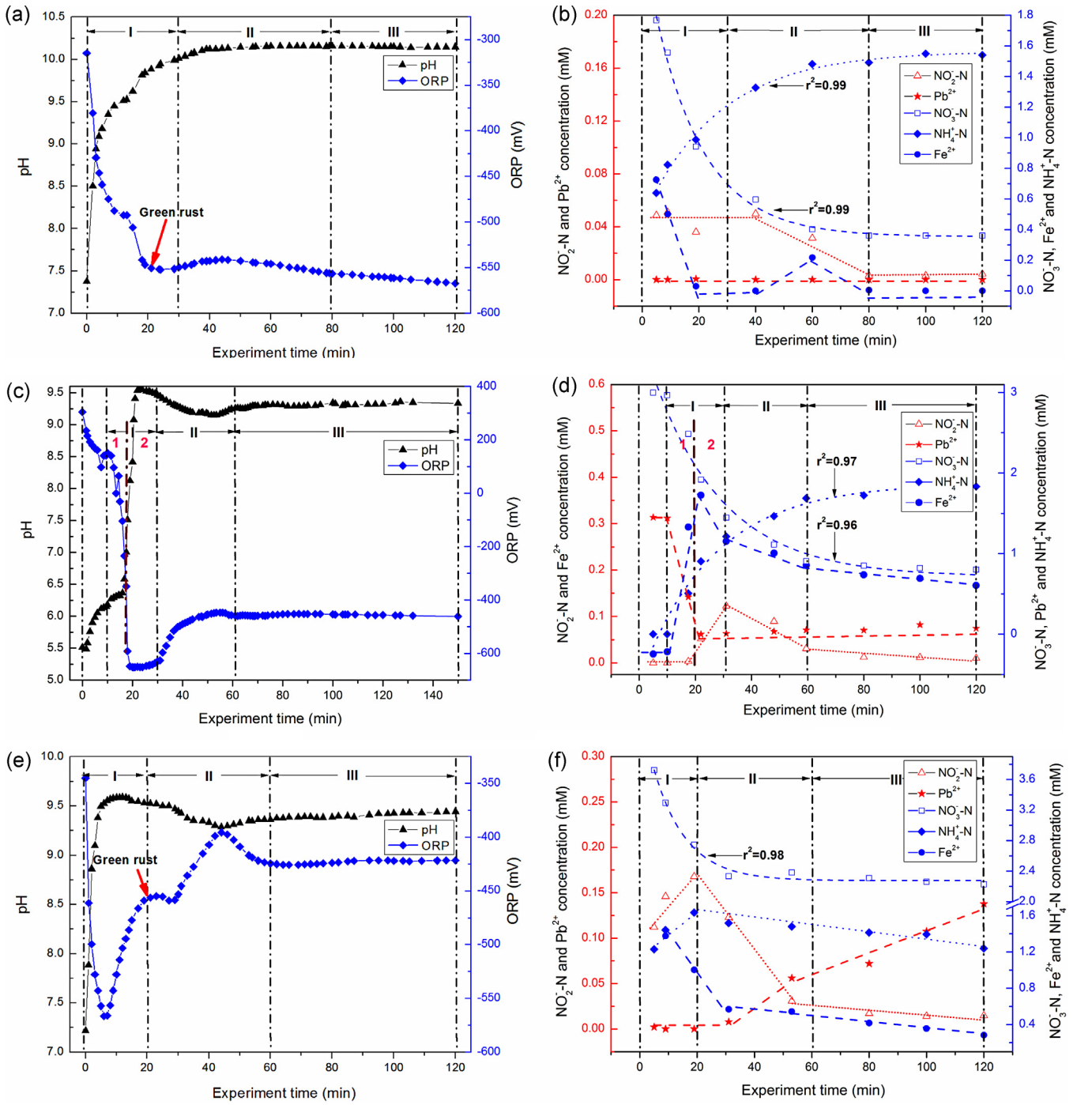

Fig. 3. (a) ORP and pH trend under excess Fe^0 conditions; (b) Pb^{2+}, Fe^{2+}, NO_3^--N, NH_4^+-N, and NO_2^--N concentrations variations under excess Fe^0 conditions; (c) ORP and pH trend under balanced Fe^0-nitrate conditions; (d) Pb^{2+}, Fe^{2+}, NO_3^--N, NH_4^+-N, and NO_2^--N concentration variations under balanced Fe^0-nitrate conditions; (e) ORP and pH trend under excess nitrate conditions; (f) Pb^{2+}, Fe^{2+}, NO_3^--N, NH_4^+-N, and NO_2^--N concentration variations under excess nitrate conditions; (nZVI, 0.5 g/L).

pH, which significantly enhanced Pb^{2+} precipitation and eventual removal from aqueous phase.

3.6. Right time to re-dose nZVI

nZVI-based remediation is commonly done via permeable reactive barriers or injection wells at remediation sites. As shown by this study, deficiency of nZVI relative to NO_3^- or other oxidizers present in soil or groundwater will lead to the remobilization of Pb^{2+}. As such, it is necessary to determine the right time to re-dose nZVI (to make it abundant relative to the oxidizer). Fig. 5b illustrates that from 0 to 60 min, ORP declined sharply after the every dosage of $Pb(NO_3)_2$, and Pb^{2+} ions were not detected in aqueous phase. However, from 60 to 100 min, rather than decrease, ORP increased continuously after the dosage of $Pb(NO_3)_2$ (due to nZVI deficiency), and an increasing amount of Pb^{2+} ions were detected in solution. When nZVI was re-dosed at 100 min, both ORP and Pb^{2+} concentration decreased significantly. Hence, decreasing ORP trend indicates deficiency of nZVI, and the right time to re-dose nZVI.

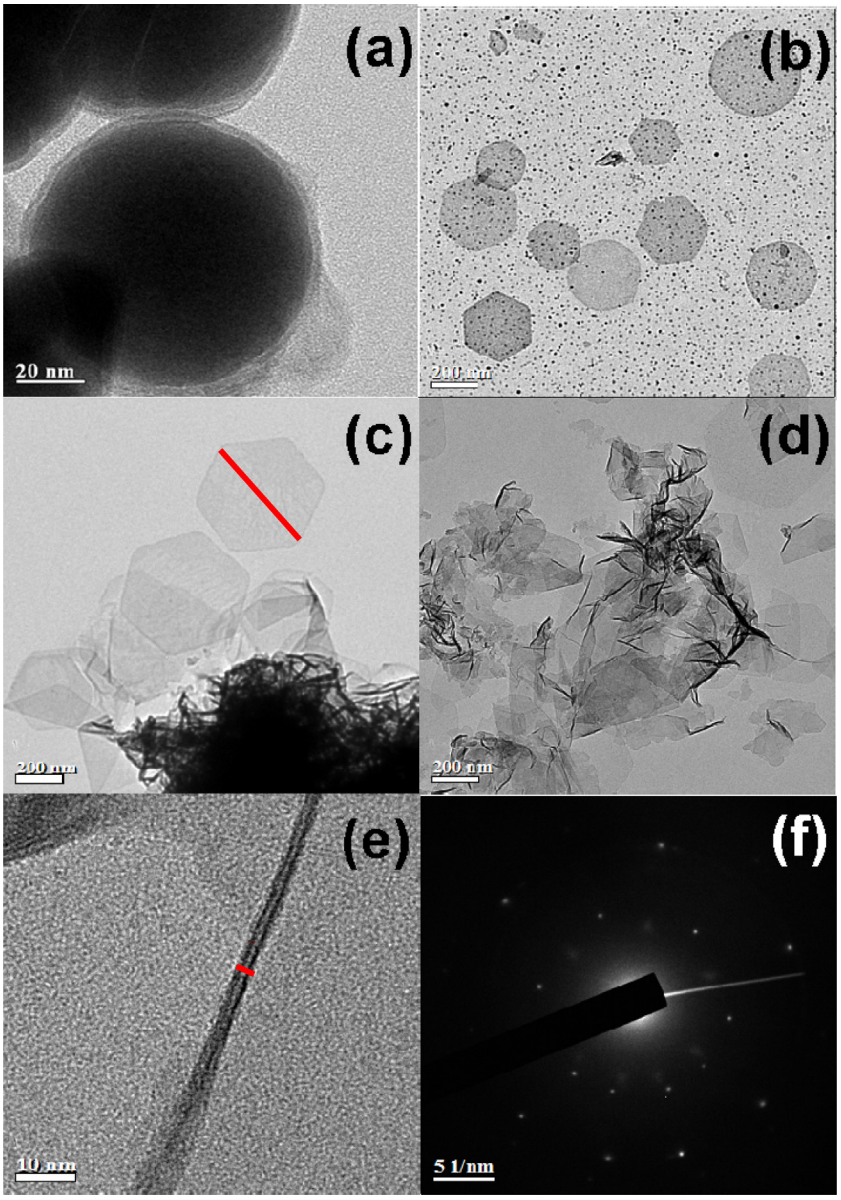

Fig. 4. TEM images of samples from excess nitrate conditions (1.93 mM nitrate). (a) Fresh nZVI; (b) nanoparticles after 10 min (phase I); (c) nanoparticles after 35 min (red line, the maximum diameter of the Pb^{2+}-containing ferrite) (phase II); (d) nanoparticles after 95 min (phase III); (e) the thickness of the Pb^{2+}-containing ferrite (red line); (f) the electron diffraction pattern of the Pb^{2+}-containing ferrite.

4. Discussion

4.1. Mechanisms of formation and transformation of Pb-containing ferrite

Formation of ferrite requires that rate of incorporation of Fe^{2+} into the ferrite crystal exceed the rate of Fe^{2+} oxidation to Fe^{3+} (Eqs. (5) and (3)) [44–46]. In this study, Pb^{2+} was not reduced to Pb^0 by nZVI (Fig. S7, no Pb^0 was detected by X-ray photoelectron spectroscopy), but it was incorporated into the ferrite crystal structure during the dehydroxylation-crystallization process. This is similar to observations by Tamaura et al. [47]. Although the large ionic radius of Pb inhibits the growth and stability of ferrite [48], and the atomic sizes of Pb and iron differ by 22.2% [49], EDS analysis confirmed that Pb-containing ferrite was formed, and the ratio of Pb to Fe in the ferrite was ~15%. The influencing factors on the formation of substitutional solid solution include electrochemical factor, relative valence effect, and crystal structure factor [48].

For the conventional ferrite process in aqueous system, favorable conditions are usually ≥60 °C and pH ≥ 11, and ferrite could be formed within 20 min [50–52]. In our study, pH was ≤10 in all conditions, but ferrite formation still occurred mainly via the GR pathway [47]. GR was also observed in excess nZVI condition but there was no ferrite formation (Fig. S6) due to Fe^{3+} deficiency. Stability of ferrite was decreased as Fe^{2+} ions in ferrite were used for nitrite reduction as Fe^0 and Fe^{2+} run out in solution (in excess nitrate conditions, Eq. (6)). Loss of ferrite led to release of co-precipitated Pb and nitrite consumption. The entire reaction is illustrated in Fig. 6. In contrast to a previous study by Reinsch et al. [53], which reported surface passivation of nZVI by nitrate, we observed rapid corrosion (oxidation) of nZVI by nitrate in this study. Acceleration oxidation of nZVI is due to stripping of the oxide shell from the Fe(0) core, which increases reactivity and surface area

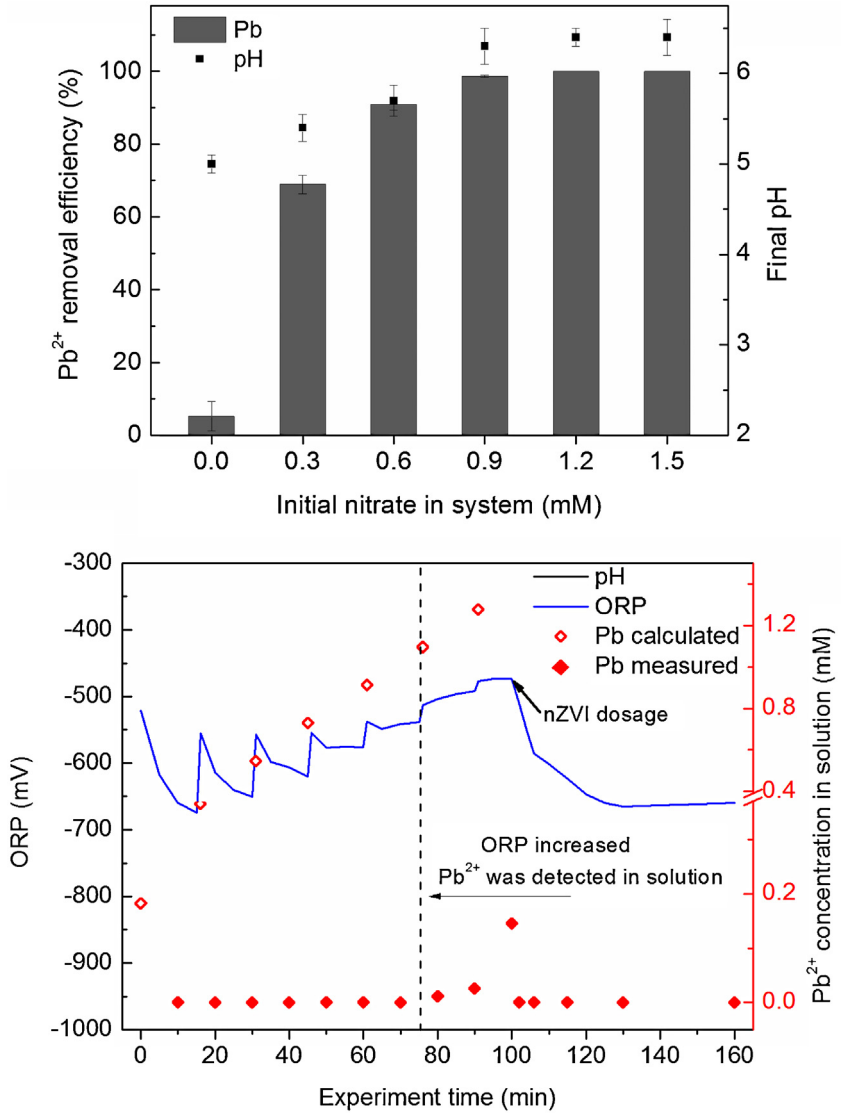

Fig. 5. (a) Nitrate effect on Pb^{2+} removal by nZVI (0.2 g nZVI/L; 1.2 mM $Pb(AC)_2$; reaction time, 20 min); (b) determining the right time to dose nZVI through ORP monitoring.—, ORP; ◊, Pb^{2+} calculated; ♦, Pb^{2+} measured.

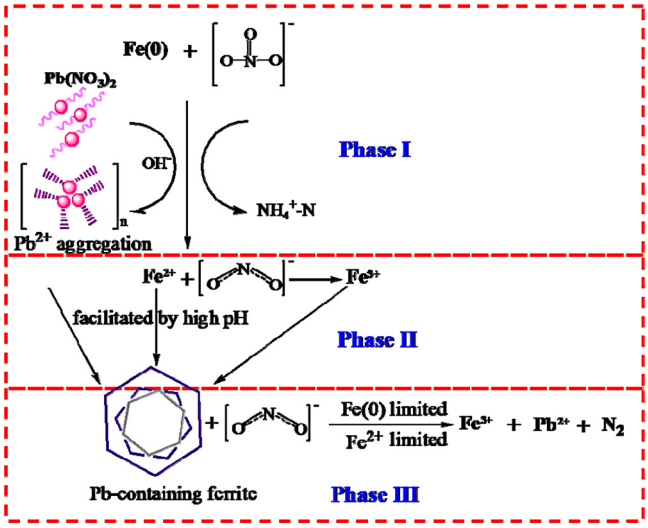

Fig. 6. Redox reaction process under excess nitrate conditions.

[19]. Oxidation by dissolved oxygen was negligible in this study due to the infinitesimal amount of oxygen compared to nitrate and the relatively short reaction time.

$$Fe^{2+} \xrightarrow{NO_3^-, NO_2^-} Fe^{3+} \quad (5)$$

$$Pb_xFe_{(3-x)}O_4 \xrightarrow{NO_2^-} xPb^{2+} + (1-x)Fe^{3+} \quad (6)$$

4.2. Relationship between ORP and the reaction among Pb^{2+}, NO_3^-, and nZVI

In batch tests to investigate the relationship between Pb^{2+} removal performance and ORP variation in $Pb(NO_3)_2$–nZVI reaction system, it seemed that there was a critical concentration of $Pb(NO_3)_2$ below which there was complete Pb^{2+} removal without remobilization, and above which Pb^{2+} was still detected in aqueous phase. According to Eq. (3) [17–19], the theoretical threshold concentration of $Pb(NO_3)_2$ to completely react with 2 g/L nZVI is 4.46 mM, which agrees with our result (Fig. 2a). ORP has a clear relationship with the redox processes in nZVI reaction system [7,38,54]. ORP mainly depends on the composition of the film formed on the

electrode and is also partially influenced by the concentrations of dissolved Fe^{2+} and H_2.

According to the ORP trend seen in Figs. 2b and 3, the reaction among Pb^{2+}, nitrate, and nZVI can be divided into three phases. In the first phase, nZVI particles attach to the ORP electrode as they are introduced into the system, forming a (visible) Fe^0 film on the electrode. This Fe^0 film results in rapid decrease in ORP. However, rapid oxidation of Fe^0 to Fe^{2+} by nitrate significantly affects ORP. Under excess nitrate conditions (>4.46 mM), the initial decrease in ORP is not as large as conditions with limited nitrate (Fig. 2b). Available nitrate leads to more Fe^0 consumption, producing additional Fe^{2+} and Fe^{3+}. Due to significant decrease in Fe^0, the composition of the film on the electrode begins to change to Fe^0–Fe^{2+}. In excess nitrate conditions, the remaining Fe^0 is so small that ORP increases quickly after an initial short period of decrease.

In the second phase, accumulated nitrite (from nitrate reduction by Fe^0) is reduced with the electrons donated by Fe^0 (in excess Fe^0 conditions) or Fe^{2+} (in excess nitrate conditions) [55]. ORP does not change much in excess Fe^0 conditions because the Fe^0 film remains on the electrode. However, under excess nitrate state, ORP increases, peaks, and then decreases, indicating a significant change in the composition of the film around the electrode. It is likely that the increase in ORP is caused by nitrite reduction, and the increase–maximum–decrease trend is caused by the difference in nitrite reduction rate. Nitrite reduction rate is accelerated by Fe^{2+} ions [55] in the second phase. Notably, this correlates with the time Fe^{2+} in ferrite is consumed, leading to ferrite deterioration and release of Pb^{2+}.

In the third phase, the remaining nitrite in the excess nitrate condition is reduced at a relatively slow rate, characterized by a moderate increase in ORP and Pb^{2+} concentration. Nitrite is not detected in the third phase of excess nZVI conditions. As indicated in this study, ORP can serve as an indicator for the transformation of nZVI, and the different redox reactions occurring in Pb^{2+}/NO_3^-/nZVI reaction system.

5. Conclusions and implications for management of Pb^{2+} remediation in the presence of nitrate

In this study, we demonstrated that Pb^{2+} removal by nZVI was significantly affected by the presence and concentrations of nitrate. Nitrate reduction by nZVI led to increase in solution pH, facilitating Pb^{2+} precipitation. However, excess nitrate (relative to nZVI) conditions were not favorable for complete Pb^{2+} removal. Apart from the change in pH, nitrate also influenced Pb^{2+} removal from the aqueous phase via the ferrite process. However, sequestration of Pb^{2+} in ferrite crystals was only temporary as the crystals were not stable under excess nitrate conditions. One potential disadvantage of nitrate reduction by nZVI is the production of toxic ammonium and nitrite ions.nZVI-based remediation can be done via permeable reactive barriers or injection wells at remediation sites. As shown by this study, deficiency of nZVI relative to an oxidizing agent (e.g. nitrate) may lead to undesirable consequences, such as remobilization of previously adsorbed pollutants (e.g. Pb^{2+}). As such, it is necessary to determine the right time to remove nZVI and immobilized Pb^{2+} (before remobilization), or re-dose nZVI (to make it abundant relative to the oxidizer)—the former being more suitable for heavy metal polluted industrial wastewater treatment, while the latter more practical for groundwater remediation. Careful ORP monitoring during nZVI-based remediation of Pb^{2+} and nitrate may provide valuable information on the status of the reaction and for determining the appropriate time to remove adsorbed pollutant or re-dose nZVI. Specifically, as seen in our study, highly negative ORP values ($\leq$−600 mV) indicated complete immobilization of Pb^{2+} ions (excess Fe^0 condition) while less negative values ($\sim$−475 mV) suggested incomplete immobilization of Pb^{2+} ions (excess nitrate conditions). Thus, continuous ORP monitoring will contribute to improving the management of nZVI-based remediation of heavy metal pollution with nitrate interference.

Acknowledgments

This work was supported by the China Scholarship Council for Yiming Su, National Natural Science Foundation of China (Nos. 51278356, 51138009, 51208365), the National Key Technologies R&D Program of China (No. 2012BAJ25B02), New Century Excellent Talents in University (NCET-11-0391), the Project of Shanghai Science and Technology Commission (No. 14XD1403700), and the Tongji University Excellent Young Talents Training Fund.

Appendix A. Supplementary data

Supplementary data associated with this article can be found, in the online version, at http://dx.doi.org/10.1016/j.jhazmat.2014.08.040.

References

[1] C. Reimann, K. Bjorvatn, B. Frengstad, Z. Melaku, R. Tekle-Haimanot, U. Siewers, Drinking water quality in the Ethiopian section of the East African Rift Valley I—data and health aspects, Sci. Total Environ. 311 (2003) 65–80.
[2] W.L. Zhang, Z.X. Tian, N. Zhang, X.Q. Li, Nitrate pollution of groundwater in northern China, Agric. Ecosyst. Environ. 59 (1996) 223–231.
[3] P.J. Squillace, J.C. Scott, M.J. Moran, B.T. Nolan, D.W. Kolpin, VOCs, pesticides, nitrate, and their mixtures in groundwater used for drinking water in the United States, Environ. Sci. Technol. 36 (2002) 1923–1930.
[4] S. Rodriguez-Mozaz, M.J. López de Alda, D. Barceló, Monitoring of estrogens, pesticides and bisphenol A in natural waters and drinking water treatment plants by solid-phase extraction–liquid chromatography–mass spectrometry, J. Chromatogr. A 1045 (2004) 85–92.
[5] J. Qiu, China faces up to groundwater crisis, Nature 466 (2010) 308.
[6] S. Yan, B. Hua, Z.Y. Bao, J. Yang, C.X. Liu, B.L. Deng, Uranium(VI) removal by nanoscale zerovalent iron in anoxic batch systems, Environ. Sci. Technol. 44 (2010) 7783–7789.
[7] Y.T. Wei, S.C. Wu, C.M. Chou, C.H. Che, S.M. Tsai, H.L. Lien, Influence of nanoscale zero-valent iron on geochemical properties of groundwater and vinyl chloride degradation: a field case study, Water Res. 44 (2010) 131–140.
[8] W.L. Yan, H.L. Lien, B.E. Koel, W.X. Zhang, Iron nanoparticles for environmental clean-up: recent developments and future outlook, Environ. Sci. Proc. Imp. 15 (2013) 63–77.
[9] D. O'Carroll, B. Sleep, M. Krol, H. Boparai, C. Kocur, Nanoscale zero valent iron and bimetallic particles for contaminated site remediation, Adv. Water Resour. 51 (2013) 104–122.
[10] Y. Su, A.S. Adeleye, Y. Huang, X. Sun, C. Dai, X. Zhou, Y. Zhang, A.A. Keller, Simultaneous removal of cadmium and nitrate in aqueous media by nanoscale zerovalent iron (nZVI) and Au doped nZVI particles, Water Res. 63C (2014) 102–111.
[11] P. Bennett, F. He, D.Y. Zhao, B. Aiken, L. Feldman, In situ testing of metallic iron nanoparticle mobility and reactivity in a shallow granular aquifer, J. Contam. Hydrol. 116 (2010) 35–46.
[12] D.W. Elliott, H.L. Lien, W.X. Zhang, Zerovalent iron nanoparticles for treatment of ground water contaminated by hexachlorocyclohexanes, J. Environ. Qual. 37 (2008) 2192–2201.
[13] J.M. Thompson, B.J. Chisholm, A.N. Bezbaruah, Reductive dechlorination of chloroacetanilide herbicide (alachlor) using zero-valent iron nanoparticles, Environ. Eng. Sci. 27 (2010) 227–232.
[14] T.B. Scott, I.C. Popescu, R.A. Crane, C. Noubactep, Nano-scale metallic iron for the treatment of solutions containing multiple inorganic contaminants, J. Hazard. Mater. 186 (2011) 280–287.
[15] X.Q. Li, W.X. Zhang, Sequestration of metal cations with zerovalent iron nanoparticles—a study with high resolution X-ray photoelectron spectroscopy (HR-XPS), J. Phys. Chem. C 111 (2007) 6939–6946.
[16] S. Klimkova, M. Cernik, L. Lacinova, J. Filip, D. Jancik, R. Zboril, Zero-valent iron nanoparticles in treatment of acid mine water from in situ uranium leaching, Chemosphere 82 (2011) 1178–1184.
[17] Z.M. Jiang, L. Lv, W.M. Zhang, Q.O. Du, B.C. Pan, L. Yang, Q.X. Zhang, Nitrate reduction using nanosized zero-valent iron supported by polystyrene resins: role of surface functional groups, Water Res. 45 (2011) 2191–2198.
[18] S. Krajangpan, J.J.E. Bermudez, A.N. Bezbaruah, B.J. Chisholm, E. Khan, Nitrate removal by entrapped zero-valent iron nanoparticles in calcium alginate, Water Sci. Technol. 58 (2008) 2215–2222.
[19] K. Sohn, S.W. Kang, S. Ahn, M. Woo, S.K. Yang, Fe(0) nanoparticles for nitrate reduction: stability, reactivity, and transformation, Environ. Sci. Technol. 40 (2006) 5514–5519.

[20] A. Ryu, S.W. Jeong, A. Jang, H. Choi, Reduction of highly concentrated nitrate using nanoscale zero-valent iron: Effects of aggregation and catalyst on reactivity, Appl. Catal. B Environ. 105 (2011) 128–135.
[21] Z. Xiong, D.Y. Zhao, G. Pan, Rapid and controlled transformation of nitrate in water and brine by stabilized iron nanoparticles, J. Nanopart. Res. 11 (2009) 807–819.
[22] Y.F. Xi, M. Mallavarapu, R. Naidu, Reduction and adsorption of Pb^{2+} in aqueous solution by nano-zero-valent iron—a SEM, TEM and XPS study, Mater. Res. Bull. 45 (2010) 1361–1367.
[23] X. Zhang, S. Lin, X.Q. Lu, Z.L. Chen, Removal of Pb(II) from water using synthesized kaolin supported nanoscale zero-valent iron, Chem. Eng. J. 163 (2010) 243–248.
[24] X. Zhang, S. Lin, Z.L. Chen, M. Megharaj, R. Naidu, Kaolinite-supported nanoscale zero-valent iron for removal of Pb^{2+} from aqueous solution: reactivity, characterization and mechanism, Water Res. 45 (2011) 3481–3488.
[25] R.A. Crane, T.B. Scott, Nanoscale zero-valent iron: Future prospects for an emerging water treatment technology, J. Hazard. Mater. 211–212 (2012) 112–125.
[26] C. Noubactep, S. Care, R. Crane, Nanoscale metallic iron for environmental remediation: prospects and limitations, Water Air Soil Pollut. 223 (2012) 1363–1382.
[27] S.C. Wong, X.D. Li, G. Zhang, S.H. Qi, Y.S. Min, Heavy metals in agricultural soils of the Pearl River Delta, South China, Environ. Pollut. 119 (2002) 33–44.
[28] J. Chen, C. Tang, Y. Sakura, J. Yu, Y. Fukushima, Nitrate pollution from agriculture in different hydrogeological zones of the regional groundwater flow system in the North China Plain, Hydrogeol. J. 13 (2005) 481–492.
[29] Y. Zhang, Y. Su, X. Zhou, C. Dai, A.A. Keller, A new insight on the core–shell structure of zerovalent iron nanoparticles and its application for Pb(II) sequestration, J. Hazard. Mater. 263 (Part 2) (2013) 685–693.
[30] X.Q. Li, W.X. Zhang, Iron nanoparticles: the core-shell structure and unique properties for Ni(II) sequestration, Langmuir 22 (2006) 4638–4642.
[31] M.Z. Kassaee, E. Motamedi, A. Mikhak, R. Rahnemaie, Nitrate removal from water using iron nanoparticles produced by arc discharge vs. reduction, Chem. Eng. J. 166 (2011) 490–495.
[32] Y.J. Tu, C.K. Chang, C.F. You, S.L. Wang, Treatment of complex heavy metal wastewater using a multi-staged ferrite process, J. Hazard. Mater. 209 (2012) 379–384.
[33] W.X. Wang, Z.H. Xu, J. Finch, Fundamental study of an ambient temperature ferrite process in the treatment of acid mine drainage, Environ. Sci. Technol. 30 (1996) 2604–2608.
[34] B. Karn, T. Kuiken, M. Otto, Nanotechnology and in situ remediation: a review of the benefits and potential risks, Environ. Health Perspect. 117 (2009) 1823–1831.
[35] B. Karn, T. Kuiken, M. Otto, Nanotechnology and in situ remediation: a review of the benefits and potential risks, Cienc. Saude Coletiva 16 (2011) 165–178.
[36] M. Spiro, Polyelectrodes: the behaviour and applications of mixed redox systems, Chem. Soc. Rev. 15 (1986) 141–165.
[37] W.-X. Zhang, Nanoscale iron particles for environmental remediation: an overview, J. Nanopart. Res. 5 (2003) 323–332.
[38] Z. Shi, J.T. Nurmi, P.G. Tratnyek, Effects of nano zero-valent iron on oxidation-reduction potential, Environ. Sci. Technol. 45 (2011) 1586–1592.
[39] D.W. Elliott, W.-X. Zhang, Field assessment of nanoscale bimetallic particles for groundwater treatment, Environ. Sci. Technol. 35 (2001) 4922–4926.
[40] S. Gandhi, B.-T. Oh, J.L. Schnoor, P.J.J. Alvarez, Degradation of TCE, Cr(VI), sulfate, and nitrate mixtures by granular iron in flow-through columns under different microbial conditions, Water Res. 36 (2002) 1973–1982.
[41] K.A. Third, M. Newland, R. Cord-Ruwisch, The effect of dissolved oxygen on PHB accumulation in activated sludge cultures, Biotechnol. Bioeng. 82 (2003) 238–250.
[42] K.B. Ayala-Luis, N.G.A. Cooper, C.B. Koch, H.C.B. Hansen, Efficient dechlorination of carbon tetrachloride by hydrophobic green rust intercalated with dodecanoate anions, Environ. Sci. Technol. 46 (2012) 4683.
[43] Y. Liu, G.V. Lowry, Effect of particle age (Fe0 content) and solution pH on NZVI reactivity: H2 evolution and TCE dechlorination, Environ. Sci. Technol. 40 (2006) 6085–6090.
[44] B.E. Morgan, O. Lahav, R.E. Loewenthal, Advances in seeded ambient temperature ferrite formation for treatment of acid mine drainage, Environ. Sci. Technol. 39 (2005) 7678–7683.
[45] B.E. Morgan, R.E. Loewenthal, O. Lahav, Fundamental study of a one-step ambient temperature ferrite process for treatment of acid mine drainage waters, Water Sa 27 (2001) 277–282.
[46] B.E. Morgan, O. Lahav, G.R. Hearne, R.E. Loewenthal, A seeded ambient temperature ferrite process for treatment of AMD waters: Magnetite formation in the presence and absence of calcium ions under steady state operation, Water Sa 29 (2003) 117–124.
[47] Y. Tamaura, T. Katsura, S. Rojarayanont, T. Yoshid, H. Abe, Ferrite process; heavy metal ions treatment system, Water Sci. Technol. 23 (1990) 1893–1900.
[48] J.A. Alonso, The factors influencing solid solubility in metallic alloys, Latin Am. J. Metall. Mater. 5 (1985) 3–13.
[49] J.C. Slater, Atomic radii in crystals, J. Chem. Phys. 41 (1964) 3199–3204.
[50] T. Sugimoto, B. Matijevic, Formation of uniform spherical magnetite particles by crystallization from ferrous hydroxide gels, J. Colloid Interf. Sci. 74 (1980) 227–243.
[51] K. Hasegawa, T. Sato, Particle-size distribution of $CoFe_2O_4$ formed by the coprecipitation method, J. Appl. Phys. 38 (1967) 4707–4713.
[52] O.P. Perez, K. Tohji, Y. Umetsu, Ambient-temperature synthesis of metal-bearing ferrites: how and why? J. Alloy Compd. 290 (1999) 129–136.
[53] B.C. Reinsch, B. Forsberg, R.L. Penn, C.S. Kim, G.V. Lowry, Chemical transformations during aging of zerovalent iron nanoparticles in the presence of common groundwater dissolved constituents, Environ. Sci. Technol. 44 (2010) 3455–3461.
[54] A. Adeleye, A. Keller, R. Miller, H. Lenihan, Persistence of commercial nanoscaled zero-valent iron (nZVI) and by-products, J. Nanopart. Res. 15 (2013) 1–18.
[55] Y.H. Huang, T.C. Zhang, Nitrite reduction and formation of corrosion coatings in zerovalent iron systems, Chemosphere 64 (2006) 937–943.